# Highly Ionized Dense Plasma in a Cesium Penning Arc

G. A. Swartz and L. S. Napoli

Citation: Physics of Fluids **8**, 1550 (1965); doi: 10.1063/1.1761452
View online: http://dx.doi.org/10.1063/1.1761452
View Table of Contents: http://scitation.aip.org/content/aip/journal/pof1/8/8?ver=pdfcov
Published by the AIP Publishing

tion becomes increasingly important and must be included in the power balance analysis.

## XIII. SUMMARY AND CONCLUSIONS

From the data presented, it is seen that, over a wide range of Ohmic heating currents, a rather satisfactory balance can be achieved between the power input and the power going into radiation, ionization, and heating. Most of the residual discrepancy early in the pulse is attributed to the use of the pulsed gas feed and the associated difficulty of obtaining a correct average of the power radiated around the discharge tube. Charge exchange losses have been estimated and shown to be small. Except possibly for very low currents ($< 2$ kA), these losses never exceed 10% of the power input.

From the close agreement of the power balance between the above quantities alone, it appears that the last term in Eq. (2)—i.e., the power loss associated with the sheath drop—must be small and, hence, can play no major role in the power balance picture. This conclusion implies, in turn, that the average energy, $\gamma \bar{E}_s$, carried per particle to the walls must be roughly comparable to the average energy, $\bar{E}$, of the plasma particles.

## ACKNOWLEDGMENTS

It is a pleasure to acknowledge helpful discussions on the subject with Dr. L. Spitzer, Dr. M. B. Gottlieb, Dr. W. Hooke, Dr. W. Stodiek, and Dr. S. Yoshikawa. We are also endebted to Elizabeth Cary for assistance in the computations and to M. Perron and his technician staff for their part in the operation of the C-Stellarator.

THE PHYSICS OF FLUIDS VOLUME 8, NUMBER 8 AUGUST 1965

# Highly Ionized Dense Plasma in a Cesium Penning Arc

G. A. SWARTZ AND L. S. NAPOLI
*RCA Laboratories, Princeton, New Jersey*
(Received 16 February 1965; final manuscript received 12 April 1965)

A stable cesium plasma with a density of $10^{15}$ ions/cm$^3$ and 50% ionization was produced by a Penning arc. A hot, high work function, anode is shown to be a significant factor in the achievement of this very dense highly ionized plasma. Plasma instabilities, which are normally present in the Penning arc, were found to be rotating in the $\mathbf{j} \times \mathbf{B}$ direction. These instabilities are damped when the arc pressure is 0.5 torr and the arc boundary is irregular. Radial and axial plasma density variations were measured. The radial density gradient decreased when the plasma became stable. The axial plasma density variation indicates that the prime source of plasma electrons is the hot cathode.

## INTRODUCTION

HIGHLY ionized quiescent cesium and other alkaline metal plasmas have been produced and studied in recent years by several groups.[1-3] In these plasmas the electrons are supplied from a hot-cathode surface, and the ions are supplied by contact ionization of neutral atoms at a nearby high work-function surface. The plasma density is a maximum when the random plasma electron current density equals the temperature-limited cathode emission. A maximum current of 10 A/cm$^2$ at the cathode surface limits the plasma density to less than $10^{14}$ ions/cm$^3$.[3]

A Phillips-Ionization-Gauge[4] configuration under arc conditions (hereafter referred to as a Penning arc) utilizes the effect of a cathode sheath which allows the random electron current density in the plasma to be less than the emitted electron current density at the cathode. Rather than utilize impact ionization for ion generation which requires high pressure and low ionization, contact ionization is provided at a fixed radius all along the plasma length by a hot, high work function, positively biased cylindrical electrode. The anode is heated to prevent reduction of the anode work function by deposition of the alkaline metal on the anode surface.[5]

In this configuration, the cathode provides electrons; the anode provides ions; the double sheath inhibits longitudinal electron and ion loss at the

[1] A. L. Eichenbaum and K. G. Hernqvist, J. Appl. Phys. **32**, 16 (1961).
[2] J. Y. Wada and R. C. Knechtli, Proc. IRE **49**, 1926 (1961).
[3] K. G. Hernqvist and J. R. Fendley, Jr., J. Appl. Phys. **34**, 979 (1963).
[4] F. Penning, Physica **3**, 873 (1936).
[5] I. Langmuir, Phys. Rev. **33**, 954 (1929).

cathode,[6] and the magnetic field inhibits electron loss radially. Thus a favorable combination of contact ionization, arc conditions, and plasma configuration yield a highly ionized dense plasma.

## TUBE CONSTRUCTION

The experimental investigation of the Penning arc was performed on three tubes which differ only in their heater configuration and a diagnostic probe configuration. Each of the tubes contained a cesium pump and feed system and the hot-cathode, hot-anode electrode configuration which is used to generate the cesium Penning arc. Schematic drawings of the three tubes are shown in Figs. 1(a)–(c). An impregnated cathode of 0.625-cm diam is positioned 0.5 cm from each end of a metal cylindrical anode. The metal cylinder, which is 2.5 cm long and 0.5 cm in diameter, is constructed of 10% tungsten–90% tantalum alloy. The cylindrical anode is indirectly heated by radiation from a current-carrying heater outside the cylinder. Cesium vapor is fed into the arc region from a heated cesium well below the arc. The cesium vapor condenses in a water cooled tube and drains back into the cesium well.

Each of the three tubes contained a cylindrical probe near the anode wall and various other diagnostic probes. Tube 1 contained 50 Gc/sec and 100 Gc/sec waveguide sections between the cathode and anodes. Tube 2 contained four tantalum probes along the arc axis and a fifth probe placed behind the cathode. The axial probes consist of tantalum bands wrapped around a 0.030 × 0.030-in. laminated alumina rod. The lead to each of the four bands passes through one of four grooves in the rod. The lead from the fifth probe behind the cathode was placed next to the alumina rod and covered with a ceramic coating. The alumina rod passes through a 0.050-in.-diam hole in the face of one of the cathodes. There is an identical hole in the face of the opposite cathode. Tube 3 contains a second cylindrical probe that was capable of movement across the diameter of the arc. The metal shield and inner conductor of the movable probe are connected to the base of the tube via a flexible lead. Another flexible lead is used to connect the probe shield to a base lead at a point approximately 1.0 in. from the base. In the presence of a magnetic field used for the arc, current is passed from one base lead to another through the probe shield. The magnetic field is perpendicular to the current direction, and the resulting $\mathbf{J}\times\mathbf{B}$ force on the probe shield moves the probe along the arc radius.

[6] M. J. Druyvesteyn, Physik **64**, 781 (1930).

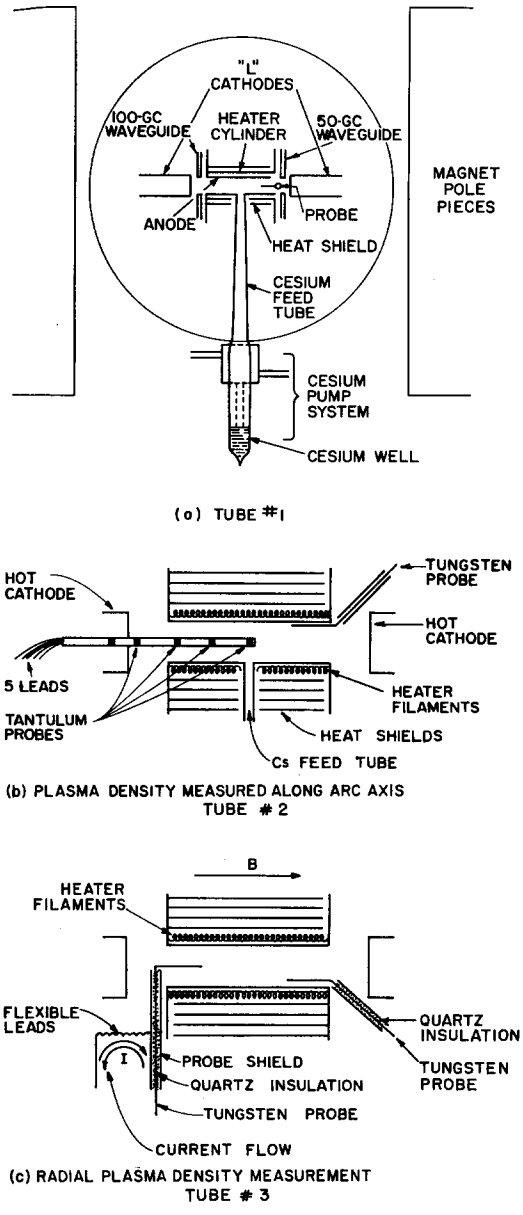


FIG. 1. Schematic of Penning arc tubes.

In Tube 1, the anode heater is a current-carrying cylinder concentric with the anode cylinder. In the other two tubes, the anode heaters are a series of ten current-carrying tungsten coils stretched along the outside of the anode wall.

## CESIUM PRESSURE MEASUREMENTS IN THE ARC REGION

Cesium flux in the arc region and, therefore, the arc pressure, were determined at various cesium well temperatures by measuring the electron emission from a hot tungsten or tantalum probe in the anode cylinder. Since the probe is radiatively heated by

the hot anode, the probe temperature is proportional to the anode temperature. The emission measurements are made in the absence of a magnetic field and with the cathodes and anode at the same potential. Comparison of the measured electron emission with the "$S$" curves measured for tungsten by Taylor and Langmuir[7] or for the tantalum by Houston[8] indicates the cesium flux. The comparison is made at the minimum of the "$S$" curve where the knowledge of the probe temperature is unnecessary.

Axial probe 2 in Tube 2 was used to measure the ratio of flux in the anode cylinder to the flux in the cesium well at various well temperatures between 250° and 300°C. Table I lists the flux ratios measured at five different cesium well temperatures. These measurements show that the flux ratio is constant at about 11 over the 50° temperature range and is in essential agreement with measurements made in tubes with a similar cesium pump system.[9]

## GENERAL PROPERTIES OF THE ARC

A typical current versus voltage curve for the Penning arc is shown in Fig. 2. The applied axial magnetic field is 5000 G. All the data shown in this report were taken in a 5000-G field except where a different value of the field is specified. The anode temperature was approximately 1900°K.

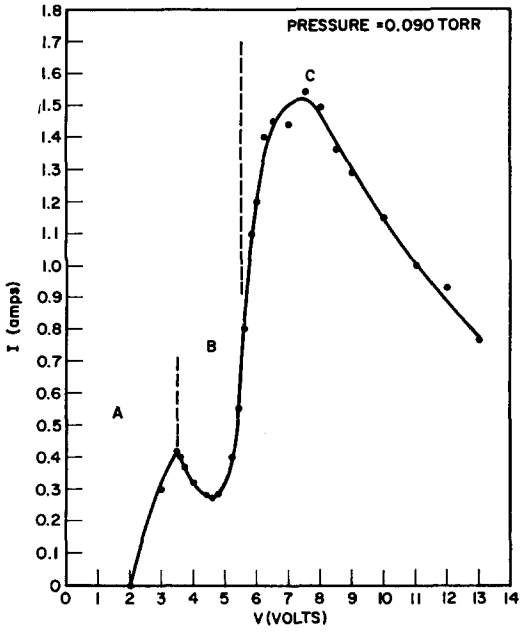


FIG. 2. Typical $I$–$V$ curve for the Penning arc.

TABLE I. Flux ratios.

| Cesium well temperature °C | $\frac{\Gamma_{well}}{\Gamma_{cyl}}$ |
|---|---|
| 257 | 11.3 |
| 272 | 10.9 |
| 281 | 10.5 |
| 245 | 12.3 |
| 303 | 9.9 |

Differences in the nature of the probe current at various arc voltages indicate that the curve in Fig. 2 can be considered in three sections. Figure 3(a) shows the probe ion current versus time oscillogram for the stable thermionic plasma which characterizes Sec. A of the curve. Figures 3(b) and 3(c) show probe ion current versus time oscillograms for the unstable plasmas which characterize Secs. B and C of the curve. The voltage source for the probe is a capacitor which is charged to $-22.5$ or $-45$ V and discharged through the plasma via the probe. The time constant of the capacitor and plasma is limited to about 100 $\mu$sec to prevent vaporization of the tungsten probe. The probe current in Fig. 3(b) shows a coherent 100-kc/sec instability which is amplitude-modulated at 5 kc/sec. This instability is very sensitive to the arc voltage and difficult to reproduce experimentally. Figure 3(d) shows that the instability is damped as the arc voltage is increased by 0.3 V.

A probe positioned at the edge of the arc indicates that the instabilities shown in Fig. 3(c) are large-amplitude density fluctuations (~80% of the maximum density) at frequencies from 50 to 250 kc/sec and small-amplitude fluctuations at frequencies between 1 and 10 mc/sec. The 50- to 250-kc/sec fluctuations are generally coherent; whereas, the high-frequency fluctuations are incoherent and appear as noise. Plasma density was measured with the edge probe when the arc pressures were sufficient to damp the instabilities.

## PLASMA DENSITY MEASUREMENTS

Plasma densities measured with the various probes show the effectiveness of the contact ionization mechanism in providing ions for the discharge. Contact ionization of cesium was used to advantage in all three Penning arc tubes. The tantalum–tungsten anode in the Penning arc tube is heated to remove cesium metal from its surface, and thereby, maintain

[7] J. B. Taylor and I. Langmuir, Phys. Rev. **44**, 423 (1933).
[8] J. M. Houston, Bull. Am. Phys. Soc. **6**, 358 (1961).
[9] G. A. Swartz and L. S. Napoli, Bull. Am. Phys. Soc. **7**, 150 (1962).

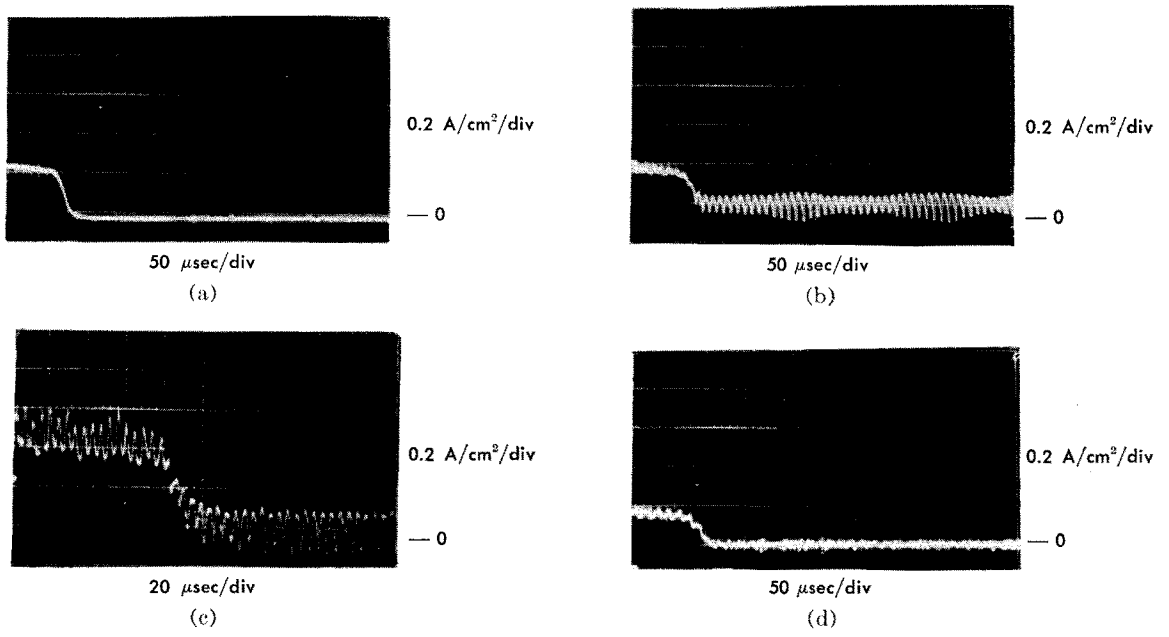


FIG. 3. Probe current versus time for various conditions in the Penning arc tube. (a) Voltage = 3 V, current = 0.3 A. (b) Voltage = 3.7 V, current = 0.37 A. (c) Voltage = 8.5 V, current = 1.36 A. (d) Voltage = 4.0 V, current = 0.32 A. Pressure = 0.09 Torr.

a high effective work function at the anode surface. An 8% coverage of tungsten by cesium reduces the work function from 4.52 to 3.9 V.[7] As the work function of the anode surface decreases below the ionization energy of cesium, the efficiency of the contact ionization mechanism drops sharply. Since the work function of tungsten (4.52 V) does not differ greatly from that of tantalum–tungsten alloy (~4.2 V), one can assume the cesium coverage on the alloy to be 8% or less for a high surface-ionization efficiency. Curve A in Fig. 4, which is a plot of measured saturation probe current in a thermionic plasma as a function of anode temperature, shows the sharp decrease in plasma density as the cesium coverage of the anode surface is increased above 8%. Curve B in Fig. 4 shows a similar decrease in the plasma density under arc conditions as the cesium coverage of the anode surface is increased above 8%. The data shown in Curve A are from Tube 3 with an arc pressure of 0.09 Torr and in Curve B are from Tube 1 with an arc pressure of 0.5 Torr.

Relative density measurements in Tube 2 provide further indication that impact ionization in the plasma volume does not generate the major portion of the plasma. Tube 2, which was designed to measure a longitudinal density profile, contained only two usable axial probes in the arc; one probe next to a cathode and another probe 1 cm from the cathode along the arc axis. The measured density at one centimeter from the cathode is 50% of the density at the cathode. If most of the plasma were generated by impact ionization in the volume, the plasma density near the cathode would be less than that in the center of the arc.[10] The radial density profile of the low pressure unstable plasma measured

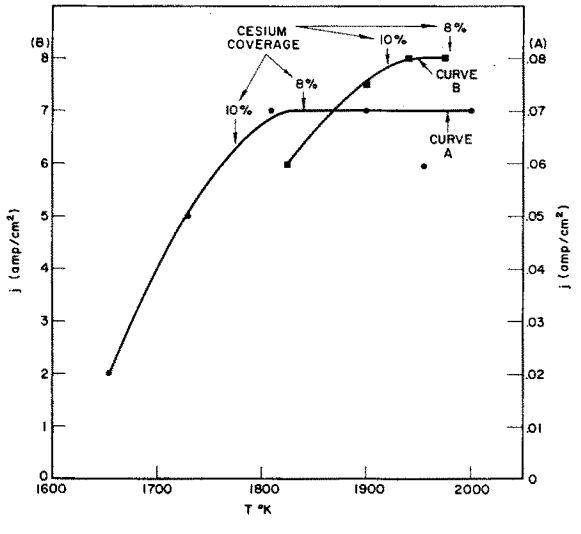


FIG. 4. (a) Saturation probe current in a thermionic plasma as a function of anode temperature. (b) Saturation probe current in a Penning arc plasma as a function of anode temperature. The Cesium coverage increases and thus anode work function decreases as the anode temperature is decreased.

[10] C. Biechler, P. Chroney, R. Maddix, and H. Madore, Record of the International Congress on Microwave Tubes, Paris, France (1964).

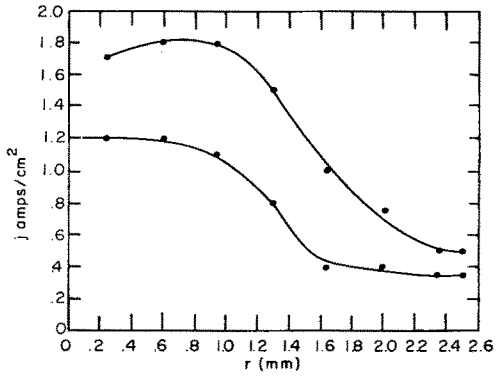


FIG. 5. Maximum and minimum ion saturation current as a function of the probe's radial position.

in Tube 3 is shown in Fig. 5. The radially movable probe not only gave information on the plasma density profile, but also provided clues on damping mechanisms of the instabilities. In the high pressure arc, as the probe was moved radially away from the plasma center, the density gradually decreased as expected. At a radius of 1.6 mm the density was 75% of maximum. At a radius of 1.8 mm (the plasma radius is 2.5 mm), the density suddenly decreased a factor of 2.3, and large fluctuations were observed on the probe. [See Figs. 6(a) and 6(b).] These could have resulted from two things. Either the plasma has two regions: one stable high density region ($r < 1.8$ mm) and an unstable low density region ($r > 1.8$ mm), or the removal of the probe constituted a boundary-condition change. It is more likely that the second explanation is correct since the anode radius (the plasma boundary) is 2.5 mm and an abrupt change in density would be expected at a radius of 2.5 mm, not at 1.8 mm. Therefore, it is concluded that the removal of the probe and supporting structure from the plasma bulk constituted a boundary condition change, and thus, the plasma as a whole became unstable.

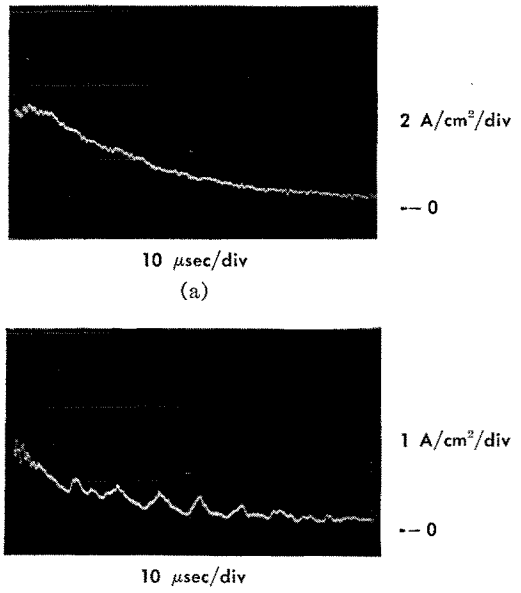


FIG. 6. Current to movable probe at two radial positions of the probe. (a) $r = 1.3$mm, pressure = 0.4 Torr, current = 1.95A. (b) $r = 2$mm, pressure = 0.5 Torr, current = 1.8A. Voltage = $7V$.

The absolute plasma density is difficult to determine because of the uncertainty in electron temperature. Typically, a cylindrical probe yielded current–voltage curves as shown in Fig. 7. Saturation ion current information but no electron temperature information was obtained from such data. The axial probes, on the other hand, yielded current-voltage curves which were exponential in nature, and, therefore, gave electron-temperature information. Since the plasma is fairly stable on the arc axis [see Fig. 8(b)], the electron temperature and plasma density determined from the axial probe is assumed to be reliable. The electron temperatures measured with the axial probe was different for different pressures and varied from 12 000°K at 0.65 Torr to 36 000°K at 0.18 Torr.

The plasma generated by an arc of 0.5-Torr pressure in Tube 1 is stable (see next section), and the I–V characteristic of a cylindrical probe in this arc is shown in Fig. 7. Since the electron temperature could not be determined from the curve, an extimate of 25 000° was made based on the axial probe measurements.

Using these data and the equation relating saturated ion current $j$, electron temperature $T_e$, one can calculate the plasma density $n$[11];

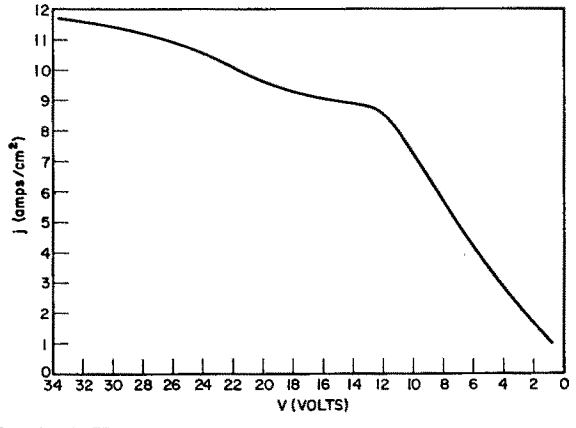


FIG. 7. $I$–$V$ characteristics for Tube 1 with an axial field of 7500 G and an arc pressure of 0.5 Torr.

[11] A. Guthrie and R. K. Wakerling, *Characteristics of Electrical Discharges in Magnetic Fields* (McGraw-Hill Book Company, Inc., New York, 1949), Chap. 2.

TABLE II. Plasma properties.

| $n$ | $T$ | Ionization (%) | Tube | Probe | Pressure (Torr) | Anode or gas and ion temp. (°K) | Saturation current ($A/cm^2$) |
|---|---|---|---|---|---|---|---|
| $4 \times 10^{14}$ | 12000° | 10 | 2 | axial | 0.65 | 1900 | 3 |
| $4 \times 10^{14}$ | 36000° | 40 | 2 | axial | 0.18 | 1900 | 4.8 |
| $8 \times 10^{14}$ | 25000°[a] | 40 | 1 | cylindrical at plasma edge | 0.5 | 1900 | 8 |
| $10^{15}$ | 25000°[a] | 50 | 1 | extrapolated to center | 0.5 | 1900 | |

[a] Estimated from lower density measurements.

$$j = 0.4ne(2kT_e/M)^{\frac{1}{2}},$$

where $e$ is electron charge, $k$ is Boltzmann's constant, and $M$ is ion mass. Table II summarizes the plasma properties.

## PLASMA INSTABILITIES

The experimental investigation of the instabilities is primarily concerned with the 50 to 250 kc/sec large-amplitude oscillations. These oscillations were observed by measuring the fluctuations in probe current, the arc current, and the light output from excited cesium ions. The experimental data indicate that the plasma instabilities are rotational instabilities of the type observed by Chen and Cooper[12] and Thomassen[13] and described by Hoh.[14]

In Tube 2 the axial probes, which were placed in the second and fourth position away from the retaining cathode, were inoperative because of breaks in the lead wires. A cylindrical probe near the anode and the remaining two axial probes, adjacent to the cathode (Probe 4) and a centimeter from the cathode (Probe 2), were used to measure the probe current oscillations. The dominant oscillation frequency is

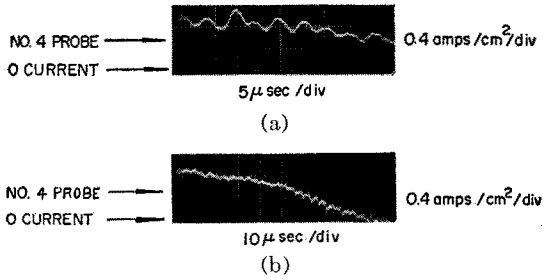


FIG. 8. Comparison of probe current fluctuations at an axial probe for anode axis (a) misaligned and (b) aligned with magnetic field. Arc conditions: Voltage = 10 V, current = 1.5 A, pressure = 0.23 Torr.

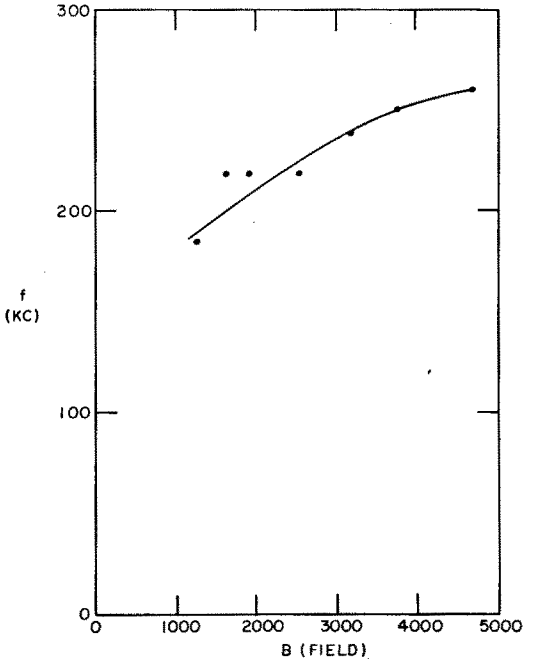


FIG. 9. Oscillation frequency as a function of the magnetic field (>1000 G). Arc conditions: Voltage = 10 V, current = 0.9–1.1 A, pressure = 0.1 Torr.

250 kc/sec in Tube 2 and 100 kc/sec in the other two tubes. The axial probe structure in Tube 2 apparently affects the oscillation frequency. The oscillation frequency at each probe of Tube 2 is the same, but the waveforms are different. Therefore, a phase relationship of the wave between the probe positions is meaningless.

Figure 8 shows the density fluctuations at Probe 4 for the anode cylinder axis misaligned with the magnetic field [see Fig. 8(a)] and aligned with the field [see Fig. 8(b)]. Misaligning the anode cylinder with respect to the magnetic field places the 4 probe off the axis of the arc. Figure 8 clearly shows that the density fluctuations at axial probe 4 increase as the probe is displaced from the arc axis.

The oscillation frequency was observed to increase

[12] F. F. Chen and A. W. Cooper, Phys. Rev. Letters 9, 333 (1962).
[13] K. I. Thomassen, Phys. Rev. Letters 14, 587 (1965).
[14] F. C. Hoh, Phys. Fluids 6, 1184 (1963).

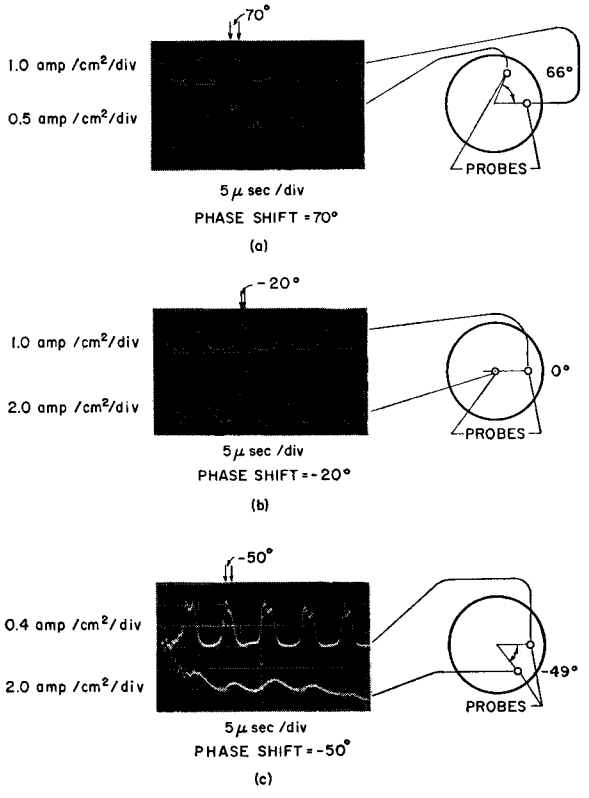


FIG. 10. Comparison of phase relationships at fixed probe and three positions of movable probe.

with increasing magnetic field as shown in Fig. 9. The plasma is stable below 1000 G. The oscillation frequency also increases with increasing arc voltage for voltages less than 10 V and is constant for arc voltages greater than 10 V.

In the third Penning-arc tube two cylindrical probes were used; one stationary and the other

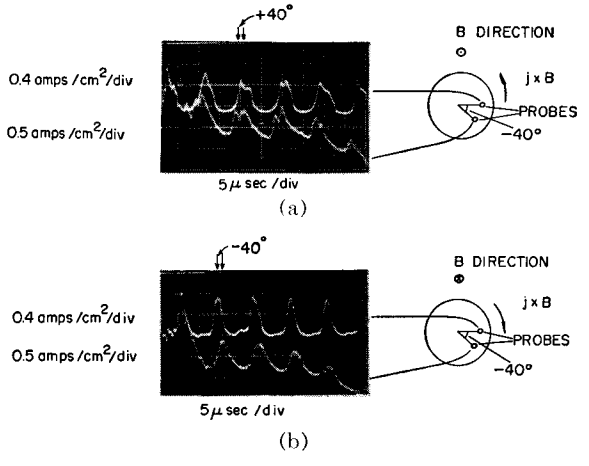


FIG. 11. Phase reversal with 180° change in magnetic field direction. Voltage = 10 V, pressure = 0.065 Torr. (a) Phase shift = +40°, current = 0.95 A. (b) Phase shift = −40°, current = 1.08 A.

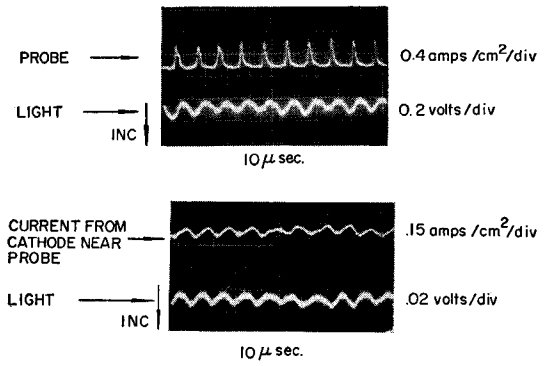


FIG. 12. Comparison of phase relationships between probe current, light output and discharge current at one end of the arc. Voltage = 10 V, current = 0.73 A, pressure = 0.035 1 Torr.

movable. The wave form of the instabilities was similar for each probe, and therefore, relative phase measurements were possible.

The instability was observed to be rotational. The ion current to each probe and the relative positions of each probe are shown in Fig. 10. When these phase measurements were made, the minimum distance between the arc axis and the movable probe was about one millimeter. The two probes are axially displaced from each other by 2.5 centimeters.

Magnetic field reversal data shown in Fig. 11 indicate a reversal in the direction of plasma rotation. The arc's radial current flow, $j$, is inward. (The electrons flow toward the cylindrical anode.) Thus Fig. 11 shows that the plasma rotates in the $\mathbf{j} \times \mathbf{B}$ direction.

Examination of Figs. 10(a)–(c) and 11 shows that the relative angular position of the movable probe with respect to the arc axis and the fixed probe follows, on a one-to-one basis, the phase relationship of the probe current fluctuations. This indicates that there is only one rotating plasma bunch.

An RCA 6199 photomultiplier, aimed at the arc cathodes, was used to measure the light output of the excited cesium ions as the arc current through each cathode was monitored. Both quantities fluctuated at the same frequency as the probe current. Figure 12 shows the probe current to the fixed probe, the current through the adjacent cathode, and the light output from the region between the same cathode and fixed probe. Figure 13 shows the positions of the high-density rotating plasma in relation to the fixed probe when both the cathode current and light output are maximum. A reversal of the magnetic field changes the sign of the phase relationship of the three quantities, and therefore, Fig. 13 also applies for a reversed field. Observation of the

arc shows that the bluish light emitted by cesium ions is most intense at the point in space where the rotating plasma is positioned when the light fluctuation is a maximum. The cathode current fluctuation may be the result of nonuniform cathode conditions. The light output fluctuations may also be the result of nonuniform cathode conditions or the asymmetric feed system for the cold cesium gas.

In Tubes 1 and 3 the instability changed modes as the arc voltage was increased. At low arc pressures two modes exist and at high arc pressures three modes exist. Frequency modes of 54, 124, and 224 kc/sec at an arc pressure of 0.31 Torr are shown in Fig. 14. At a pressure of 0.035 Torr the highest frequency mode is not observed. Comparison of the phase relationships between the two probe currents indicates that below 125 kc/sec only one plasma bunch is in rotation. Above 125 kc/sec the data are not sufficient to draw a conclusion.

At arc pressures greater than 0.4 Torr the plasma instabilities are damped if the plasma boundary has some irregularities. As the position of the movable probe in Tube 3 was changed from near the center of a high pressure arc to the edge, the amplitude of the instabilities increased. The probe current shown in Fig. 6 for a high pressure indicates the presence of a stable plasma when the probe is 1.3 mm from the arc center and a moderately unstable plasma when the probe is 2.0 mm from arc center. In Tube 1 the waveguide sections protruding into the arc provided the boundary irregularities, and stability was achieved at an arc pressure of about 0.5 Torr. In Tube 2, where the outside arc boundary is smooth, large incoherent plasma instabilities were present even at an arc pressure of 0.65 Torr.

To summarize the above results, the following statements can be made: (1) The plasma is rotating about the arc axis in the $\mathbf{j} \times \mathbf{B}$ direction. (2) The rotational velocity increases with increasing magnetic field. Below 1000 G the plasma is stable. (3) At low arc voltage ($<10$ V), the rotational velocity increases with increasing arc voltage. (4) Three frequency modes of the rotational instability

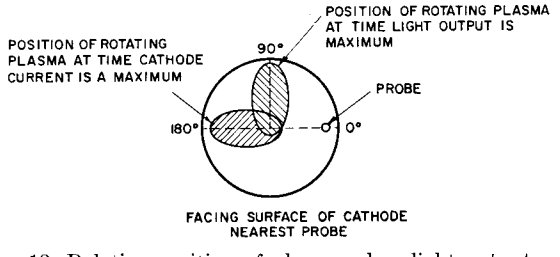


FIG. 13. Relative position of plasma when light output and cathode current are at a maximum.

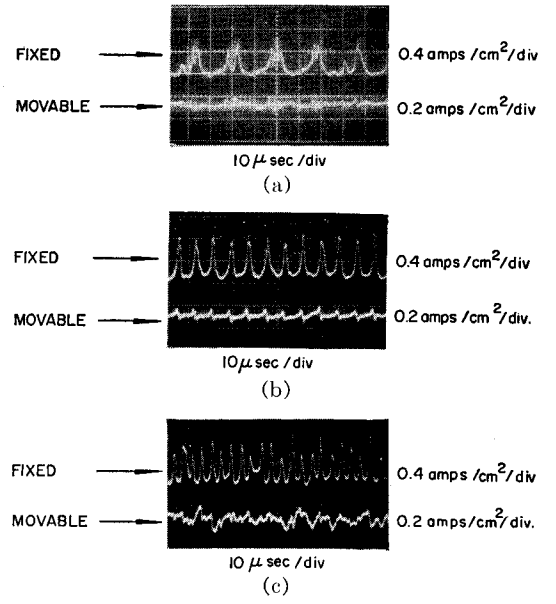


FIG. 14. Instability modes at three frequencies. High pressure arc (0.31 Torr). (a) Voltage = 4.6 V, current = 0.78 A, oscillation frequency = 54 kc/sec. (b) Voltage = 5.6 V, current = 1.2 A, oscillation frequency = 124 kc/sec. (c) Voltage = 7.3 V, current = 1.42 A, oscillation frequency = 224 kc/sec.

are observed. The arc voltage and pressure determine the dominant mode. (5) The suppression of the rotational instability is dependent on the arc pressure and the radial boundary conditions in the arc. (6) The fluctuating light intensity and cathode current are the result of the rotating plasma interacting with boundaries such as the cathode. (7) At rotational frequencies less than 125 kc/sec, only the $m = 1$ rotational mode exists.

## DISCUSSION

Hoh's treatment of the plasma motion in a Penning arc shows that the plasma becomes unstable at magnetic fields greater than a critical value.[14] The plasma drifts in the azimuthal or $\theta$ direction because of the radial electric field, $E_r$, and axial magnetic field, $B_z$, present in the plasma. The ions, which experience collisions with the neutral atoms, lag behind the electrons, and the charge separation produces an electric field in the $\theta$ direction. The azimuthal electric field in combination with the axial magnetic field causes the plasma to move outward from the axis and amplify the initial density perturbation. If the magnetic field is sufficiently weak, plasma particles can diffuse into the perturbed region and neutralize the space charge before the perturbation grows. Under these conditions, the plasma remains stable. For the plasma conditions described in Fig. 9, the measured critical magnetic field is 1000 G. A

quantitative comparison with the theory is not possible because the theory assumes zero ion current from the anode.

The velocity of the rotation, $v_\theta$, is

$$v_\theta = \omega r_0 = E_r/B_z ,$$

where $\omega$ is the angular rotational frequency and $r_0$ is the anode radius. For $B_z = 5000$ G and $r_0 = 0.25$ cm, the radial field varies from 0.4 V/mm at $\omega/2\pi = 50$ kc/sec to 2 V/mm at $\omega/2\pi = 250$ kc/sec.

The rotational instability is suppressed when the arc pressure is about0.5 Torr, and irregular boundary conditions are present at the arc's periphery. At this arc pressure an ion collides with a neutral cesium atom several times during one rotational cycle. From the mobility data of Chen and Raether[15] on cesium ions in cesium vapor, the ion–neutral collision frequency for a neutral atom density of $10^{15}$ atoms/cm$^3$ is 1.8 mc/sec. For a rotational frequency of 100 kc/sec, $\omega/\nu = 0.7$. The ion gas forces the neutral gas to drift, and this drift creates a frictional power loss at the arc boundary. The more irregular the boundary, the greater the frictional loss. When the frictional power loss becomes greater than the power available for generation of the rotational instability, the instability is suppressed.

[15] C. L. Chen and M. Raether, Phys. Rev. **128**, 2679 (1962).

## CONCLUSIONS

The hot-cathode, high work function anode Penning arc is capable of producing a stable cesium plasma with a density of $10^{15}$ ions/cm$^3$ and 50% ionization. The high work function of the anode cylinder in this arc is responsible for the high plasma density and high percentage of ionization. The observed plasma instabilities are rotational and are generated by the $\mathbf{j} \times \mathbf{B}$ forces in the plasma. These instabilities are damped when the ion-neutral collision frequency is about equal to the rotational frequency, provided irregular boundary conditions are present to inhibit the smooth flow of gas.

## ACKNOWLEDGMENTS

The authors wish to thank M. Glicksman and K. G. Hernqvist for their many helpful suggestions during the course of the work. We wish to express our gratitude to R. E. Chamberlain for his flawless assembly work on the various experimental tubes.

The research reported here was sponsored by the Electronic Technology Division of the Air Force Avionics Laboratory, Research and Technology Division, Air Force Systems Command, Wright–Patterson Air Force Base, Ohio, under contract number AF33(657)-11069, and RCA Laboratories, Princeton, New Jersey.